FUNDAMENTAL UNDERSTANDING OF HELICOPTER ROTOR HUB VIBRATION REDUCTION USING NON-STRUCTURAL LUMPED MASSES

Rohin Kumar Majeti, German Aerospace Center (DLR), Hamburg, Germany
Anil Yasasvi Turumella, German Aerospace Center (DLR), Braunschweig, Germany

Abstract

Significant potential exists for reducing the vibratory hub loads generated by the rotor through optimal blade design process. An optimization study was carried out to reduce the vibratory rotor hub loads using non-structural lumped masses and twist. The lumped masses had both spanwise and chordwise location variability. Prior to the optimization, a sensitivity analysis was carried out to understand the effect of the individual parameters on the vibration index. A significant observation from the study was that a lumped mass which was placed near the tip region and aft of the elastic axis reduces the vibration index the most. Optimally locating three lumped masses along with optimal twist led to a reduction of vibration index by 65% from the baseline case. Such a significant reduction was achieved without resorting to radical design or geometries and without expensive techniques.

1. NOTATION

Symbols	
cg, CG	Center of gravity
sc, SC	Shear center
ac, AC	Aerodynamic center
R	Radius of the rotor blade
VI	Vibration index
w_F, w_M	Weighting factors for hub forces and moments
F_{4x}, F_{4y}, F_{4z}	Rotor hub 4/rev forces, N
M_{4x}, M_{4y}, M_{4z}	Rotor hub 4/rev moments, Nm
M_1, M_2, M_3	Magnitudes of the lumped masses, kg
X_1, X_2, X_3	Radial locations of the lumped masses, m
$\theta_{\text{coll}}, \theta_{\text{cos}}, \theta_{\text{sin}}$	Rotor control angles

2. INTRODUCTION

2.1. General

The helicopter rotor serves as the primary mechanism for generating lift, propulsion, and control in helicopters. Operating within a complex and dynamic aerodynamic environment, the rotor blades rotate at high speeds. The interaction between the blades and this aerodynamic environment is the primary cause of vibration. Although other factors such as engine and transmission contribute to vibration, their effects are typically localized. Helicopter vibration refers to the oscillatory response of the helicopter airframe to forces and moments exerted by the rotor hub. The main rotor's vibratory hub loads are the primary source of vibration. These loads are transmitted to the fuselage through the rotor hub, and reducing them is expected to decrease the overall vibration level experienced by the helicopter. Vibration has significant implications for helicopter performance parameters such as maximum flight speed, fatigue, and passenger comfort. Therefore, mitigating vibration is essential for optimizing helicopter performance and ensuring a comfortable ride for passengers.

Depending on the flight regime, different phenomena contribute to significant vibratory loads on the rotor blades. At low advance ratios and during descending flight blade-vortex interaction is a primary source of high vibration levels. At higher advance ratios, the main cause of vibratory loads is the large elastic twist deformation of the blades, driven by unsteady transonic pitching moments near the blade tips. In conditions of high thrust, dynamic stall becomes the dominant source of vibration, characterized by flow separation on the retreating side of the rotor. Therefore, an effective design for reducing vibration must consider the vibration characteristics across the entire flight envelope.

2.2. Literature review

There are two approaches to reduce vibration. The first approach is through suppression techniques. These techniques can be passive or controlled actively. Active techniques work according to the measured vibration on the helicopter and try to reduce vibratory loads by generating opposing airloads (Ref. 1). However, these are expensive and complicated methods. The passive techniques, on the other hand, do not require any actuation and most of them try to reduce vibrations after the vibratory loads are generated. However, they incur a weight penalty and are also tuned for only a specific operating condition (Ref. 2). The second approach is through design process optimization where the structural and aerodynamic properties of the blade are tailored to achieve a predetermined objective. This approach has the advantage over the previous methods of decreasing vibration at the source.

There is a significant potential for reducing the vibratory hub loads generated by the rotor through blade design. For example, spanwise and chordwise distributions of blade mass result in changes in mode shapes, frequency and coupling between bending and torsional response. These could result in reduction of vibratory loads. In Ref. 3, it is theorized that the primary effect of chordwise mass distribution is to produce a twisting of the blade, as a result of coupling with the blade bending motion, and thereby to produce a cyclic airload that affects the dynamic bending response of the blade.

Blade modal shaping, frequency placement, structural and aerodynamic coupling, intermodal cancellation and modal damping were identified as factors that influence blade vibratory airloads in Refs. 4 and 5. In Ref. 4, blade twist is also given as a factor which affects vibratory hub loads in two ways. It not only modifies the basic airloads on the blades but also intensifies the interaction between flatwise and edgewise movements.

Placing the CG forward of the AC can be expected to reduce the root forces and hence the vibratory loads because of the coupling between the torsional and flapping response (Refs. 4 and 5). This also has the additional benefits of preventing blade instability (Ref. 6) and providing stability augmentation for the helicopter flight dynamics by increasing pitch damping (Ref. 7).

Adding non-structural lumped masses along the spanwise and chordwise locations of the blade is a design process method that aims to reduce the hub vibrations by manipulating the dynamic behaviour of the blade. Ref. 8 concludes that use of nonstructural mass, added in the out-board segment of the blade and in the vicinity of the blade elastic axis, is a very useful device for reducing vibration levels.

Optimization methods are very popular in multi-disciplinary engineering applications. Helicopter operation has strong aerodynamic and structural dynamics interactions and so aeroelastic optimization has been applied to rotor blade design since long (Ref. 9). The design space for rotors is frequently non-convex and may contain numerous local minima. Gradient-based optimization algorithms may become trapped at a local minimum point. Non-gradient methods such as genetic algorithms (GA) have proven invaluable due to their capability to locate global minima and accommodate the use of discrete design variables (Ref. 10). There have been optimization studies in the past which have successfully achieved reduced hub vibratory loads by employing lumped masses to move blade natural frequencies away from resonance frequencies (Refs. 11, 12). Ref.11 also states that the lumped mass in the tip is typical of rotor blades and is used to keep the mass center forward of the aerodynamic center, a common design practice to prevent torsion-flutter in rotor blades.

The effects of non-structural masses on the 4/rev hub loads were studied in Ref. 13. It was concluded that the significant reductions in these loads were the results of the addition of nonstructural mass aft of the elastic axis near the blade tip, and forward of the elastic axis around the mid-span. Through stiffness and nonstructural mass distributions, a 60-90 percent reduction in all six 4/rev hub loads is achieved for a four-bladed soft-in-plane rotor. In Ref. 14, the authors optimized non-structural tuning masses to minimize vertical shear forces. They analytically optimized the locations and mass values of multiple tuning masses and compared them with test data. These modifications tailor the mode shapes to achieve orthogonality to the airloading thereby reducing the generalized force and subsequently the hub shear. Reference 15 posited that the blade natural frequency placement is more important for hub shear reduction than the modal shaping. Minimum vibratory hub shear could be obtained by placing the tuning masses on the blade tip with a low mass penalty.

In Ref. 10, genetic algorithms were introduced to rotorcraft multidisciplinary optimization. They formulated a weighted sum of vertical vibratory hub loads as the objective function, subject to various design constraints, with tuning masses included as design variables. To reduce computational cost of the optimization process, surrogate-model based design optimization was introduced in Ref. 16. The design variables consisted of non-structural masses along with the cross-sectional dimensions of the structural members of the blade.

In Ref.s 17 and 18, lumped masses at predetermined spanwise antinode locations were used as design variables to reduce hub vibratory loads successfully. In these references, it is seen that rotor-induced vibration reduction can be addressed through either direct hub loads minimization approach or the indirect natural frequency separation approach. In contrast to the natural frequency separation approach, the hub loads minimization approach offers the advantage of addressing vibratory loads originating from aerodynamic factors.

In most of the previous studies, the spanwise location of the lumped masses were taken as design variables but not the chordwise offsets. The chordwise offsets of the lumped masses are expected to produce coupling between the torsional and flapwise bending response of the blade. Vibration reduction can be realized by taking advantage of these couplings.

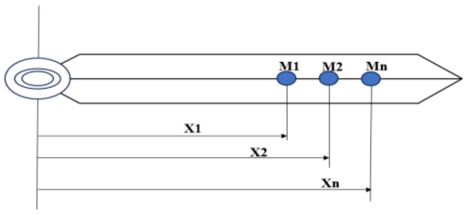

Figure 1. Design Variables of masses and placed at different locations on the helicopter rotor blade (Ref. 14)

3. PROBLEM DEFINITION

3.1. General

The current study employs three non-structural lumped masses (Fig. 1) with variations in both spanwise and chordwise directions to reduce the vibratory hub loads. The underlying mechanisms behind this reduction of the vibration are investigated. In addition, the effect of varying the geometrical twist of the blade is also studied. The study is set up as an optimization problem where the vibration index is minimized for the design variables related to the lumped masses. VAST, a multi-physics, multi-model simulation program, is used as the helicopter comprehensive analysis tool (Ref. 19). Optimization is carried out within the Remote Component Environment (RCE) which is an in-house developed workflow-integration tool (Ref. 20). A variant of the Genetic Algorithm was used as the optimizer. The HART II rotor blade and the operating condition detailed in Ref. 21 and summarized in Table 1 are used as the reference. The operating condition is a low-speed forward descent case.

Table 1. Rotor blade geometry and operating conditions

Characteristic	Value
Rotor geometry	
Rotor radius, m	2
Blade chord, m	0.121
Number of blades	4
Linear twist per span, deg	-8
Rotor solidity	0.077
Precone, deg	2.5
Airfoil	NACA23012 (trailing edge tab)
Rotor type	Hingeless
Operating conditions	
Rotational speed, rad/s	109.12
Rotor shaft angle of attack, deg	4.5
Advance ratio	0.151
Rotor thrust, N	3300
Rolling moment, Nm	20
Pitching moment, Nm	-20

3.2. Trim tool

The VAST solver integrates models from multiple physical domains, including structural dynamics, aerodynamics, and control systems, by linking their inputs and outputs. Using this coupled system, it carries out various tasks such as equilibrium analysis, modal analysis, time integration, and wind tunnel trim. The rotor blades are modelled as multi-body based finite elements.

The aerodynamic model is derived from blade element theory, with the aerodynamic discretization independent of the structural discretization. Each blade is divided into 20 aerodynamic elements, starting at a radial station of r/R=0.22. The span of these elements decreases toward the blade tip to maintain equal ring areas. Steady airloads on each element are computed using a semi-empirical analytical model based on the NACA23012 airfoil. For simplicity, tip loss is modeled by reducing lift beyond r/R=0.97. The rotor inflow is represented by a Generalized Dynamic Wake model, incorporating 6 azimuthal harmonics and 6 radial polynomials (Ref. 22).

Wind tunnel trim is performed through a sequential time simulation of a full rotor revolution, with an azimuthal step size of 15°. The trim algorithm adjusts the control angles $\theta_{\text{coll}}, \theta_{\text{cos}}, \theta_{\text{sin}}$ to meet the specified trim objectives: rotor thrust T, rotor roll moment M_x, and rotor pitch moment M_y. Simultaneously, the periodicity of the flexible rotor blades and the main rotor inflow model is verified, ensuring their values and time derivatives are the same at the start and end of the revolution. The flight condition being trimmed represents steady descent flight. In the wind tunnel configuration, this is modeled by a freestream velocity of $v_\infty = (-32.9, 0, 0)^{\text{T}}\ \text{m/s}$ in the inertial frame, with a rotor shaft angle of $\alpha = 4.5°$.

For the hub vibration problem, the vibration index (VI, Ref. 13) defined as follows was taken as the objective function

Objective function for hub vibration:

$$\boldsymbol{VI} = \boldsymbol{w_F}\sqrt{(\boldsymbol{F_{4x}})^2 + (\boldsymbol{F_{4y}})^2 + (\boldsymbol{F_{4z}})^2} + \boldsymbol{w_M}\sqrt{(\boldsymbol{M_{4x}})^2 + (\boldsymbol{M_{4y}})^2 + (\boldsymbol{M_{4z}})^2} \qquad \textbf{(1)}$$

In the above equation, the two parts on the right-hand side are composed of the 4/rev hub forces and the 4/rev hub moments multiplied by weighting factors which are taken as 1 for the current study. The forces are nondimensionalized by the required thrust (T) and the moments are nondimensionalized by R*T, where R is the radius of the blade.

4. SENSITIVITY STUDIES

Sensitivity analysis is essential in structural optimization, as it helps assess the robustness of a design. It reveals how each design variable impacts the property of interest. Initially, a set of design of experiments (DoE) were carried out to understand the effects of the lumped mass magnitude, spanwise location and chordwise location on the vibration index (VI). Figure

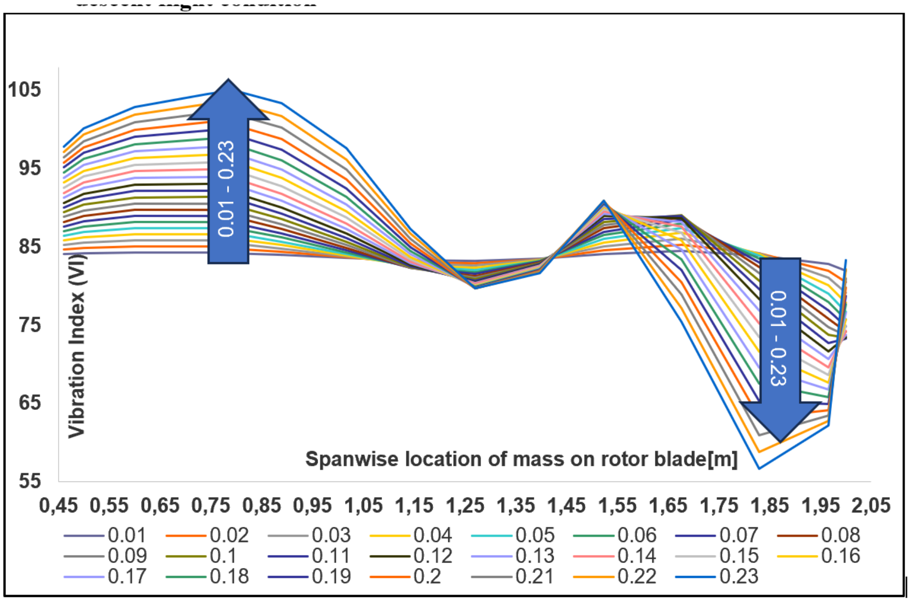

Figure 2. Vibration index variation with varying mass in increments of 0.01kg at varying spanwise location

2 shows the results of one such DoE carried out by varying a single lumped mass from 0.01kg to 0.23kg (10% of blade weight) in incremental steps of 0.01kg. The spanwise location of the lumped mass is varied from 0.45m to 2m. It is seen that there is a clear trend in the variation of the vibration index with spanwise location of the lumped mass. This trend is maintained irrespective of the magnitude of the lumped mass. The maximum VI is observed at about 0.80m or 40% span of the blade while the least VI is observed at about 1.83m or 92% span. It is interesting to note that the first location is nearly aligned with the antinode location of the second mode and the second location is closely aligned with the node locations of first, third and fifth mode, respectively.

Another set of sensitivity study was carried out to understand the behavior of vibration index with lumped masses placed at an offset from the elastic axis. A couple of plots are given in Fig. 3 and Fig. 4 whereby single masses of 0.02kg, 0.1kg and 0.23kg were placed at 0.80m and 1.83m with offset range of -0.0060m to +0.0060m. This offset range corresponds to -5% to 5% chord length.

It is seen from Figs. 3 and 4 that irrespective of the mass magnitudes, the vibration index decreases as the mass moves from aft of the elastic axis to forward

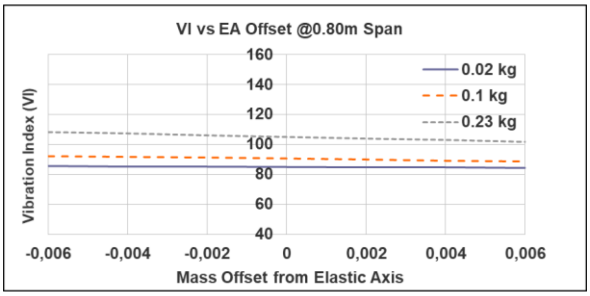

Figure 3. Vibration index Vs Elastic axis offset of mass placed at 0.80m location

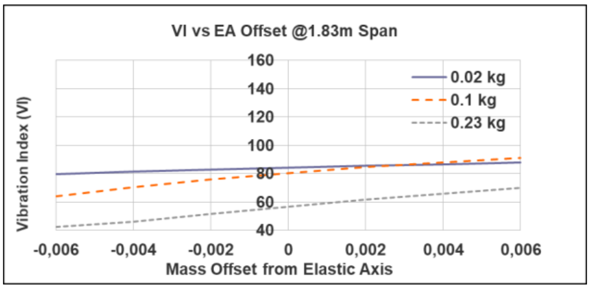

Figure 4. Vibration index Vs Elastic axis offset of mass placed at 1.83m location

offsets in the inboard location (0.80m). On the contrary, the vibration index increases as the mass moves from aft of the elastic axis to forward offset in the outboard location (1.83m). Combining the results of Figs. 2-4, it could be concluded that a lumped mass placed aft of the elastic axis near the tip region would result in a much lower vibration index than the baseline. This is in line with the findings in Ref. 13.

In addition to the lumped masses, blade twist was another parameter whose effect on the vibratory loads was studied. Figure 5 shows the results of a sensitivity analysis involving blade twist and vibration index. The twist angle was varied from -16 deg to 8 deg. It may be noted that the baseline blade twist angle is -8 deg. While the value of VI for the baseline blade is low at 83.5, it reduces further to 61.9 at a blade twist angle of -11 deg.

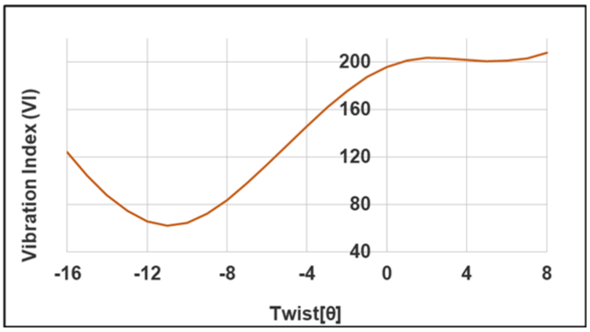

Figure 5. Vibration index Vs Blade twist angle

5. OPTIMIZATION RESULTS

The objective of the optimization studies was to obtain a combination of lumped mass magnitudes, their spanwise and chordwise locations and twist that would result in the least vibration index. The vibration index for the baseline HART II blade (BL) was found to be 83.5. Based on the earlier results, three cases were taken up for optimization as follows:

- Case I (Exp01): 3 lumped masses were placed at distinct spanwise locations on the elastic axis.
- Case II (Exp02): 3 lumped masses were placed at distinct spanwise and chordwise locations on the blade.
- Case III (Exp03): same as Case II; however, with blade twist as an additional design variable.

All the design variables used and their lower and upper bounds are summarized in Table 2.

Table 2: Design variables for the optimization

Parameters	Lower Bound	Upper Bound
Mass 1 [kg]	0	0.05
Mass 2 [kg]	0.025	0.075
Mass 3 [kg]	0.05	0.1
Location 1 [m]	0.46	2
Location 2 [m]	0.46	2
Location 3 [m]	0.46	2
EA offset 1 [m]	-0.006	0.006
EA offset 2 [m]	-0.006	0.006
EA offset 3 [m]	-0.006	0.006
Twist, θ [deg]	-16	8

For representative purpose, only the convergence plot of the objective function during the optimization process of Exp02 is shown in Fig. 6. It can be seen that there is a smooth convergence over around 800 iterations. Table 3 gives a summary of the results for the three optimization cases. The converged values of the objective function and the relevant design variables are shown.

Table 3: Summary of the results for the three optimization cases

Parameters	Exp01	Exp02	Exp03
VI	65.9	44.1	28.9
Mass 1 [kg]	0.034	0.049	0.037
Mass 2 [kg]	0.068	0.074	0.067
Mass 3 [kg]	0.084	0.094	0.089
Location 1 [m]	1.97	1.68	1.68
Location 2 [m]	2.00	1.83	1.89
Location 3 [m]	1.68	1.97	1.97
EA offset 1 [m]	-	-0.0056	0.0025
EA offset 2 [m]	-	-0.0048	0.0058
EA offset 3 [m]	-	-0.0051	-0.0038
Twist, θ [deg]	-	-	-11

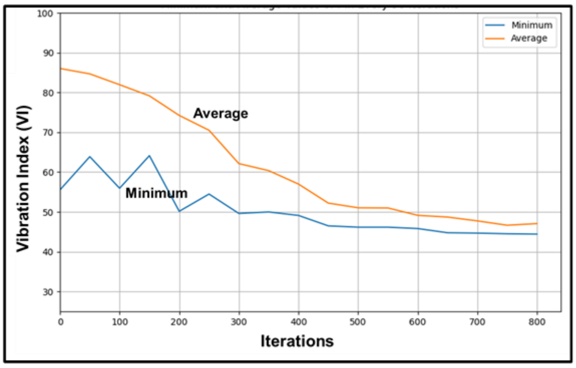

Figure 6. Convergence plot of the vibration index for Exp02

It is seen that all the three masses are located near the tip region for all the three cases. The total lumped mass magnitudes for Exp01, Exp02 and Exp03 come out to 0.186kg, 0.217kg and 0.193kg. From Exp02 result, it could be seen from the negative offsets that all the three lumped masses are placed aft of the elastic axis. This is in line with what was observed in the sensitivity studies as well. With the increase in the blade geometric twist to -11deg for the Exp03 case, we see the influence of twist in the optimal offset of the lumped masses. In this case, the largest mass of 0.089kg is placed the most outboard and aft of the elastic axis while the other masses are placed forward of the elastic axis. The reduction in vibration index achieved for the three cases with respect to the baseline case was 21%, 47% and 65% respectively. The plot of vibration indices for the three cases can be seen in Fig. 7.

A look at the 4/rev hub forces and moments in Fig. 8 shows that except for the vertical shear, all the other components for Exp01 and Exp02 have reduced

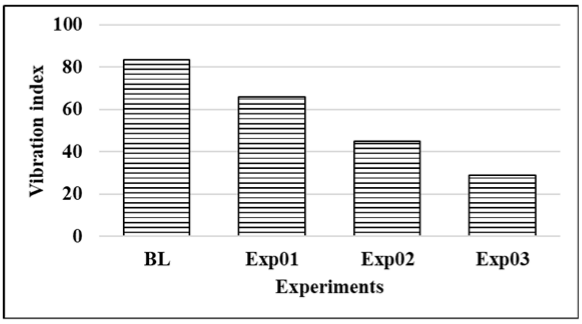

Figure 7. Comparison of the vibration index for the baseline vs optimization cases

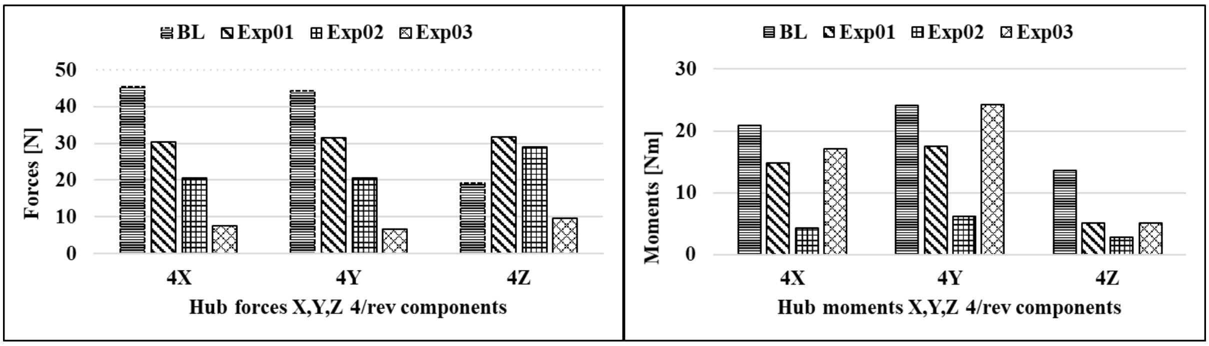

Figure 8. Comparison of the hub 4/rev force and moment components for baseline and optimization iterations

when compared to the baseline case. For Exp03 case, while all the force and moment components are less than the baseline case, the lateral and longitudinal moments are higher than those of the Exp01 and Exp02. These observations could be understood from the Campbell diagrams and mode shapes for the three cases.

In general, in the design of rotors, the natural frequencies of the blades are to be placed away from the integral multiples of the design rotor speed frequencies. Coincidence or near-coincidence of the blade natural frequencies with the multiples of rotor frequencies results in resonance conditions. The farther the blade natural frequencies are from these values, the vibratory loads also are reduced. Figures 9-11 compare the Campbell diagram of the helicopter baseline rotor blade with those of the three optimized rotors. The frequencies of interest are the second flap, second lag and the first torsion modes.

In Figure 9, it is seen that the second flap frequency for Exp01 (3 masses with no offsets) is placed farther away from the 3/rev than that for the baseline case. For Exp02 (3 masses with elastic axis offset), as seen in Figure 10, the second flap frequency is even further away from the resonance frequency. This could partly explain the reduction in vibration index from the baseline to Exp01 to Exp02. The 4/rev pitch and roll moments in the fixed hub frame are affected by the 3/rev flapwise moment. For Exp03 (Exp02 + additional geometric twist), as seen in Figure 11, the second flap frequency hasn't changed much from that of Exp02 indicating less influence of the additional geometric twist on this frequency.

Another contribution to the change in the hub vibratory loads can be observed from the mode shape diagrams. Mode shape changes result in change of the generalized forces on the rotor beam and this also influences the hub loads. Generalized forces depend on the forcing aerodynamic loading also, however this will not be examined in the current work. Figure 12 shows the mode shape of the second flap frequency for the baseline blade and that of Exp01 while Fig. 13 shows the same for Exp02. It is seen that there is a clear change in the shape as well as a shift in the node location from the baseline to Exp01 and Exp02. The difference in the mode shapes between Exp01 and Exp02 are highlighted in Figure 14. It is to be noted that the root flap bending moment of the blade translates to the pitch and roll moments in the hub-fixed coordinate system. The 4/rev pitch and roll moments get contributions from 3/rev flap bending moments.

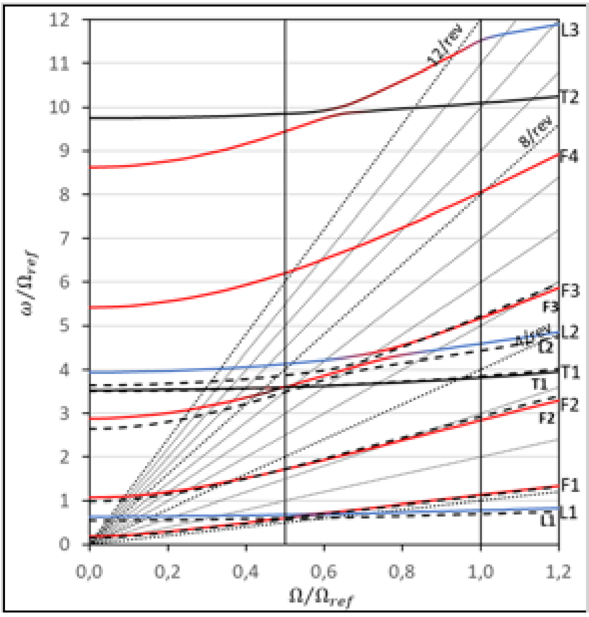

Figure 9. Campbell diagram for Exp01 juxtaposed with first six frequencies of the baseline blade

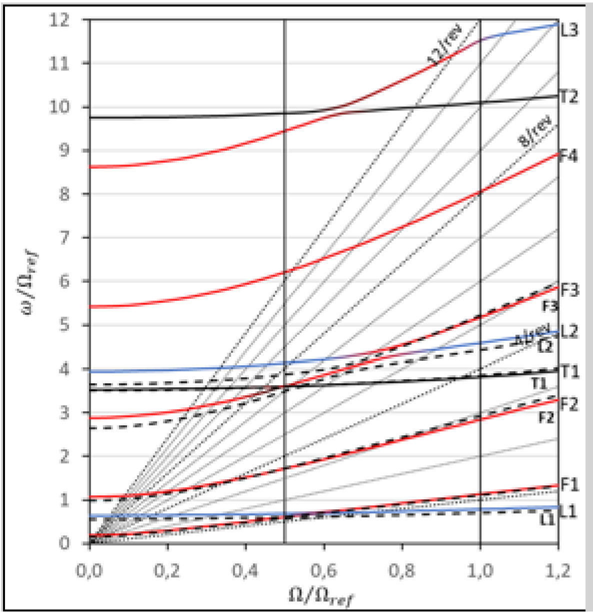

Figure 10. Campbell diagram for Exp02 juxtaposed with first six frequencies of the baseline blade

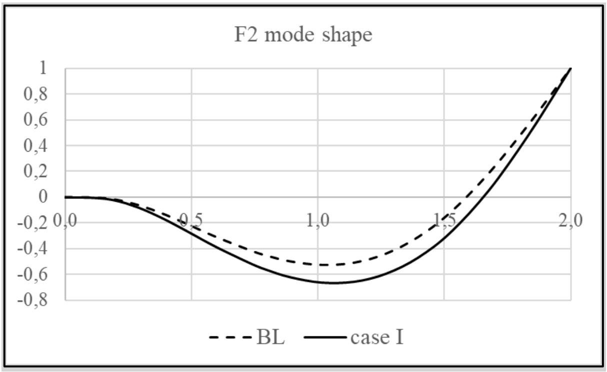

Figure 12. Mode shapes of the second flap frequency for the baseline blade vs Exp01

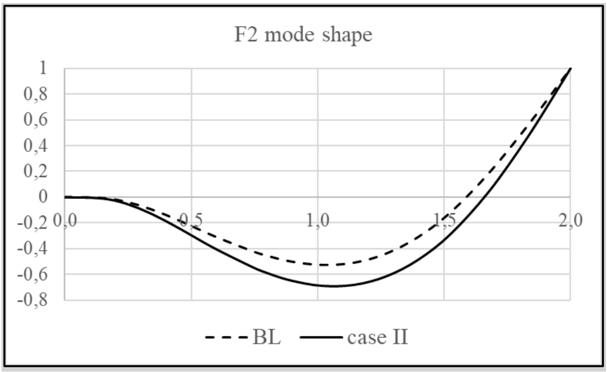

Figure 13. Mode shapes of the second flap frequency for the baseline blade vs Exp02

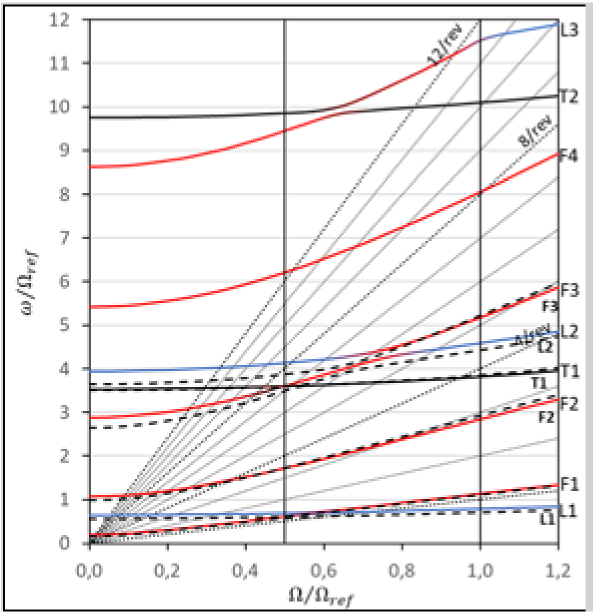

Figure 11. Campbell diagram for Exp03 juxtaposed with first six frequencies of the baseline blade

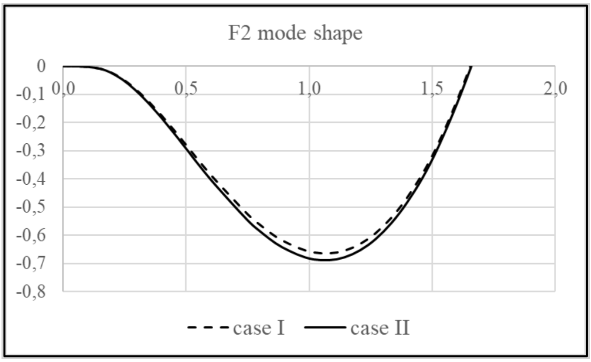

Figure 14. Comparing the mode shapes of the second flap frequencies for Exp01 and Exp02

6. CONCLUSIONS

The goal of the current work was to obtain a rotor blade configuration which has less hub vibratory loads than the baseline HART II blade using passive techniques like addition of non-structural lumped masses along spanwise and chordwise locations. The following important observations were made:

1. Sensitivity studies indicated that a lumped mass which was placed near the tip region and aft of the elastic axis reduces the vibration index the most.
2. Subsequent optimization case with three lumped masses placed at multiple spanwise and chordwise locations supported the above observation with the vibration index reducing by 47% from the baseline case level. Among the individual hub load 4/rev components, except for the vertical shear, all of them showed a reduction in values from those of the baseline case.
3. Sensitivity studies showed that negative geometric twist supports the lowering of vibration index.
4. Introducing the optimal twist to the lumped mass case resulted in a further reduction of the vibration index. The combined effect lowered the VI by 65% from the baseline case.
5. The spanwise and chordwise placement of a lumped mass affects the natural frequencies. Offsetting the critical natural frequencies away from resonance frequencies lowers the vibration index.
6. The spanwise and chordwise placement of the lumped mass also affects the mode shapes of the rotor blade. Mode shape changes result in change of the generalized forces on the rotor beam and this also influences the vibration index.

Author contact:

Rohin Majeti, rohin.majeti@dlr.de

7. REFERENCES

1. Straub, F. K., and Byrns, E.V., “Application of Higher Harmonic Blade Feathering on the OH-6A Helicopter for Vibration Reduction,” *NASA Contractor Report*, NASA-CR-4031, 1986
2. R. G. Loewy. “Helicopter Vibrations: A Technological Perspective,”. *Journal of the American Helicopter Society*, 29(4):4 – 30, October 1984.
3. Hirsch, H., Hutton, R.E. and Rasumoff, A., “Effect of spanwise and chordwise mass distribution on rotor blade cyclic stresses,” *Journal of the American Helicopter Society*, *1*(2), 1956, pp.37-45.
4. Blackwell, R. H., "Blade design for reduced helicopter vibration," *Journal of the American Helicopter Society* 28.3 (1983): 33-41. DOI: 10.4050/JAHS.28.33
5. Taylor, Robert B. *Helicopter rotor blade design for minimum vibration*. No. NASA-CR-3825. NASA, 1984.
6. Bielawa, R.L., *Rotary Wing Structural Dynamics and Aeroelasticity*, AIAA, Washington DC, USA, 1992.
7. Johnson, W., *Rotorcraft Aeromechanics*. Vol. 36. Cambridge university press, 2013.
8. Friedmann, P. P., and Shanthakumaran, P., "Optimum design of rotor blades for vibration reduction in forward flight." *Journal of the American Helicopter Society* 29.4 (1984): 70-80.
9. Chopra, I., “Design and Analysis Trends of Helicopter Rotor Systems,” *Sadhana*, Vol. 19, June 1994, pp. 427–466. DOI: 10.1007/BF02812163.
10. Lee, J., and Hajela, P., “Parallel Genetic Algorithm Implementation in Multidisciplinary Rotor Blade Design,” *Journal of Aircraft*, Vol. 33, No. 5, 1996, pp. 962–969. DOI: 10.2514/3.47042
11. Peters, D. A., Rossow, M. P., Korn, A., and Ko, T., "Design of Helicopter Rotor blades for Optimum Dynamic Characteristics." *Computers & Mathematics with Applications*, Vol. 12, (1), Jan. 1986, pp. 85-109. DOI: 10.1016/0898-1221(86)90089-1.
12. Chattopadhyay, A., and Walsh, J. L., “Technical Notes: Minimum Weight Design of Helicopter Rotor Blades with Frequency Constraints,” *Journal of the American Helicopter Society*, Vol. 34, No. 4, Oct. 1989, pp. 77-82. DOI: 10.4050/JAHS.34.77.
13. Lim, J., W., and Chopra, I., "Aeroelastic optimization of a helicopter rotor," *Journal of the American Helicopter Society*, Vol. 34, (1), Jan. 1989, pp. 52-62. DOI: 10.4050/JAHS.34.1.52

14. Pritchard, J. I., and Adelman, M. H., “Optimizing Tuning Masses for Helicopter Rotor Blade Vibration Reduction including Computed Air loads and Comparison with Test Data”, *NASA Technical Memorandum*, AVSCOM Technical Report, January 1992

15. Kim, J.-E., and Sarigul-Klijn, N., "Elastic-dynamic rotor blade design with multiobjective optimization." AIAA Journal, Vol. 39, (9), Sept. 2001, pp. 1652-1661. DOI: 10.2514/2.1512

16. Glaz, B., Friedmann, P. P., and Liu, L., “Surrogate based optimization of helicopter rotor blades for vibration reduction in forward flight,” *Structural and Multidisciplinary Optimization*, 35.4 (2008): 341-363. DOI: 10.1007/s00158-007-0137-z

17. Majeti, R. K., and Becker, F., “Surrogate-model based Optimization Framework for the Structural Design of Helicopter Rotor Blades subject to Dynamics and Failure Criteria”, Proceedings of the 79th VFS Annual Forum, West Palm Beach, FL, USA, May 2023.

18. Majeti, R. K., Becker, F. and Weiss, F., “Cross-Sectional Sizing of Rotor Blades with Dynamics and Strength Constraints”, Proceedings of the 6th Decennial VFS Aeromechanics Specialists’ Conference, Santa Clara, CA, USA, Feb 2024.

19. Hofmann, J., Weiss, F., and Mindt, M., “A New Approach to Comprehensive Rotorcraft Aeromechanics Simulation,” 77th Annual Forum of the Vertical Flight Society, Online, May 2021.

20. Boden, B., et al. "RCE: an integration environment for engineering and science." *SoftwareX*, 15, July 2021: 100759.

21. van der Wall, B. G., Lim, J. W., Smith, M. J., Jung, S. N., Bailly, J., Baeder, J. D., & Boyd, D. D., "The HART II International Workshop: An Assessment of the State-of-the-Art in Comprehensive Code Prediction," *CEAS Aeronautical Journal*, Vol. 4, July 2013, pp. 223-252. DOI: 10.1007/s13272-013-0077-9

22. He, C.,"Development and Application of a Generalized Dynamic Wake Theory for Lifting Rotors,“ *Dissertation*, Georgia Institute of Technology, 1989.